AJNR Am J Neuroradiol 20:1044–1048, June/July 1999

Case Report

Clinical Use of Diffusion-Tensor Imaging for Diseases Causing Neuronal and Axonal Damage

Aziz M. Uluğ, David F. Moore, Aviva S. Bojko, and Robert D. Zimmerman

Summary: Diffusion-tensor imaging is an emerging technique that can supply microscopic structural information about tissue in vivo. With this technique it is possible to measure the amount of anisotropy of water diffusion within tissues and to assess the degree to which directionally ordered tissues have lost their normal integrity. This study was performed in four patients to evaluate the feasibility of applying this technique in clinical situations in which there is known or suspected damage to white matter tracts.

MR diffusion imaging uses the incoherent motion of water molecules for tissue contrast. The displacement caused by the incoherent motion during imaging is on the order of micrometers. In routine practice, diffusion imaging is used to assess overall changes in the degree of diffusion (diffusion-weighted imaging and apparent diffusion coefficient maps). With these techniques, the effects of tissue anisotropy are intentionally eliminated. At this scale, the motion of water molecules is affected by the tissue microstructure, which in turn determines the degree of anisotropy. It is possible to obtain diffusion-sensitive images (diffusion-tensor imaging) in which this directional information is measured. This technique can therefore be used to study white matter fiber tracts, which are highly ordered and have distinct directions.

Description of the Technique

Subjects were studied with a 1.5-T whole-body MR unit equipped with high-performance gradients (GE Echospeed, Milwaukee, WI) using the manufacturer-supplied quadrature head coil. In addition to the standard imaging protocols (T1-weighted, T2-weighted, fluid-attenuated inversion-recovery [FLAIR], and contrast-enhanced T1-weighted sequences), we used a diffusion-tensor pulse sequence previously developed and reported by one of the authors, which can measure the diffusion in any arbitrary direction (1, 2) and is based on a single-shot, multisection, spin-echo, echo-planar imaging pulse sequence. Imaging parameters for the diffusion protocol included 6000/100 (TR/TE), a 128 × 128 matrix, 3- to 5-mm-thick interleaved data acquisition, with approximately 30 sections to cover the whole brain. Using this sequence, we collected the diffusion-weighted images in six or seven directions (x, y, z, $x+y$, $x+z$, $y+z$, $x+y+z$) in order to calculate the six independent components of the diffusion tensor. The maximum b-value used with a single gradient was 84,000 s/cm^2. The data acquisition time for the diffusion part of the examination ranged from 5 to 10 minutes depending on the number of diffusion-weighted images (eight to 28) acquired.

The images were transferred to a workstation (Sun Microsystems, Mountain View, CA). Using a multivariate fitting routine written in C, we calculated six diffusion maps corresponding to the six independent elements of the diffusion tensor. From these diffusion maps, we calculated an orientationally invariant average diffusion map (D_{av} = Trace $\{\overline{\overline{D}}\}/3$) and an orientationally invariant anisotropy map using anisotropy index UA_{surf}. This anisotropy index is calculated by comparing the D_{av} with the D_{surf}, which is a new diffusion constant obtained from the surface of the diffusion ellipsoid (3). The anisotropy index is defined in terms of diffusion constants as follows:

$$UA_{surf} = \sqrt{\left(\frac{D_{surf}}{D_{av}} - 1\right)^2} \quad \text{where}$$

$$D_{av} = (D_{xx} + D_{yy} + D_{zz})/3 \quad \text{and}$$

$$D_{surf} = \{(D_{xx}D_{yy} + D_{xx}D_{zz} + D_{yy}D_{zz} - D_{xy}D_{xy} - D_{xz}D_{xz} - D_{yz}D_{yz})/3\}^{1/2}$$

The diffusion anisotropy index UA_{surf} is scaled from 0 to 1, where 0 corresponds to isotropic diffusion and 1 to fully anisotropic diffusion. We compared the measured diffusion constant and the anisotropy values of the diseased tissue with values obtained from healthy volunteers and, where appropriate, compared them with the patient's contralateral side.

Case Reports

Case 1

A 50-year-old patient with amyotrophic lateral sclerosis (ALS) confirmed by electromyography and EL ESCORIAL criteria (4), was imaged. Routine pre- and postcontrast MR findings were normal, with the exception of a small left-sided frontal white matter focus of hyperintensity, consistent with a nonspecific focus of demyelination.

Figure 1 shows the average diffusion constant map (D_{av}) with regions of measurements indicated by boxes. Table 1 summarizes the diffusion measurements. The diffusion anisotropy map revealed decreased anisotropy in the anterior aspect of the posterior limb of the internal capsule (PLIC) (just posterior to the genu) bilaterally in the area of the corticospinal tract (CST). The diffusion anisotropy measurement (UA_{surf}) of the anterior portion of the PLIC was 0.10 on the left side and 0.12 on the right side. The measured diffusion anisotropy of the posterior portion of the PLIC and the adjacent white matter

Received September 30, 1998; accepted after revision February 22, 1999.

From the Departments of Radiology (A.M.U., R.Z.) and Neurology (D.F.M., A.S.B.), Cornell University Medical College-New York Presbyterian Hospital, New York.

Address reprint requests to Aziz M. Uluğ, PhD, Department of Radiology, Box 141, Cornell University Medical College, 1300 York Ave, New York, NY 10021.

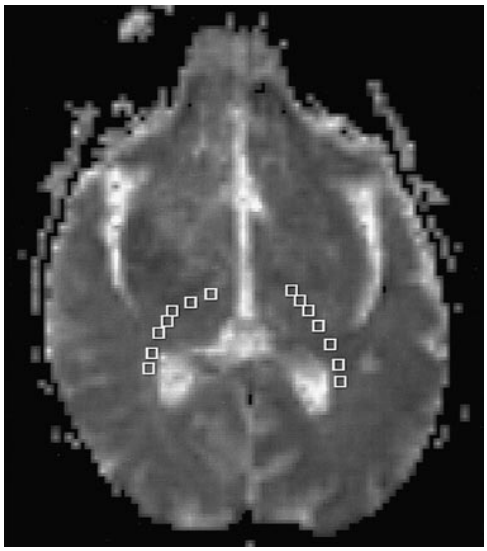

FIG 1. Diffusion map D_{av} shows the regions of interest (*boxes*) in the PLIC and adjacent white matter. Regions of interests were placed from posterior to anterior. Results of the measurements are summarized in Table 1.

was 0.20 on the left side and 0.21 on the right side. The normal diffusion anisotropy of the PLIC and adjacent white matter, previously measured in five volunteers using the same pulse sequence (3), was 0.19 ± 0.03. The 50% bilateral decrease of the diffusion anisotropy in the anterior portion of the PLIC is consistent with microscopic damage, with loss of the normal directionality of water movement.

Average diffusion constant measurements were not informative. The D_{av} measured from the left PLIC and adjacent white matter was 0.66 ± 0.04 10^{-5} cm^2/s. There were no significant differences between the posterior and the anterior portions of the PLIC. On the right, D_{av} was slightly greater (0.72 ± 1.5 10^{-5} cm^2/s), with a larger deviation of diffusion constants. Our previous study showed that normal D_{av} in the PLIC and adjacent white matter is 0.69 ± 0.30 10^{-5} cm^2/s (3).

Case 2

A 71-year-old patient with a large infarct of the right middle cerebral artery distribution was imaged 18 months after the onset of infarction. Hyperintensity typical of wallerian degeneration was seen on long-TR images extending through the posterior limb of the right internal capsule through the right cerebral peduncle and the right ventral pons along the expected course of the right CST. The D_{av} and diffusion anisotropy UA_{surf} of the CST were measured from the PLIC to the cervical spinal cord (15 axial sections, 12 in the brain and three in the spinal cord at 75 mm). At each level, the right side was compared with the left in the expected location of the CST. The data are tabulated in Table 2 and displayed graphically in Figure 2. Figure 3 is a sagittal image showing the locations of the axial sections.

The fiber tracts superior to the spinal cord on the right (ipsilateral to the stroke) had decreased diffusion anisotropy as compared with the left side. The mean diffusion anisotropy, obtained by averaging the measurements superior to the spinal cord, was 0.17 for the ipsilateral side and 0.23 for the contralateral side (26% decrease). Below the pyramidal tract decussation, in the spinal cord, the average diffusion anisotropy from the three inferior sections was 0.51 on the right (ipsilateral to the infarct) and 0.46 on the left (contralateral), corresponding to a 10% decrease of diffusion anisotropy of the contralateral fiber tract. The signal-to-noise ratio was decreased in the cervical cord as compared with the brain, reflecting the small size of the cord and the signal drop-off at the inferior portion of the imaging coil.

A detailed look at the data (Fig 2) reveals that it is possible to follow the damaged right CST for about 60 mm, from the infarction to the spinal cord. The measured average diffusion constant (22% increase) was elevated on the right side. The diffusion anisotropy images quantified the damage in the fibers

TABLE 1: Diffusion tensor measurements of the posterior limb of the internal capsule (PLIC) and adjacent white matter in ALS patient*

Region of Interest	Left Side		Right Side	
	D_{av} (10^{-5} cm^2/s)	UA_{surf}	D_{av} (10^{-5} cm^2/s)	UA_{surf}
Posterior 1	0.71	0.24	0.86	0.24
2	0.68	0.15	0.76	0.23
3	0.60	0.21	0.75	0.16
4	0.72	0.16	0.73	0.15
5	0.62	0.11	0.54	0.10
6	0.66	0.09	0.50	0.16
Anterior 7	0.64	0.10	0.90	0.12
Average ± SD (regions 1 to 7)	0.66 ± 0.04	0.15 ± 0.06	0.72 ± 0.15	0.16 ± 0.05
Average ± SD for posterior horn of PLIC and adjacent white matter (regions 1, 2, 3)	0.66 ± 0.06	0.20 ± 0.04	0.79 ± 0.06	0.21 ± 0.04
Average ± SD for anterior parts of PLIC (regions 5, 6, 7)	0.64 ± 0.02	0.10 ± 0.01	0.65 ± 0.22	0.12 ± 0.03

* Normal values for this region are D_{av} = 0.69 ± 0.03 10^{-5} cm^2/s and anisotropy index UA_{surf} = 0.19 ± 0.03 (3).

TABLE 2: Average (± SD) measurements following corticospinal white matter tract in patient (case 2) with wallerian degeneration secondary to right hemispheric stroke 18 months after ictus (diffusion anisotropy index [UA_{surf}] is normalized between 0 and 1)

	Ipsilateral		Contralateral	
	D_{av} (10^{-5} cm^2/s)	UA_{surf}	D_{av} (10^{-5} cm^2/s)	UA_{surf}
Above pyramidal decussion	0.98 ± 0.20	0.17 ± 0.15	0.80 ± 0.13	0.23 ± 0.16
Spinal cord	1.43 ± 1.03	0.51 ± 0.12	1.30 ± 0.19	0.46 ± 0.17

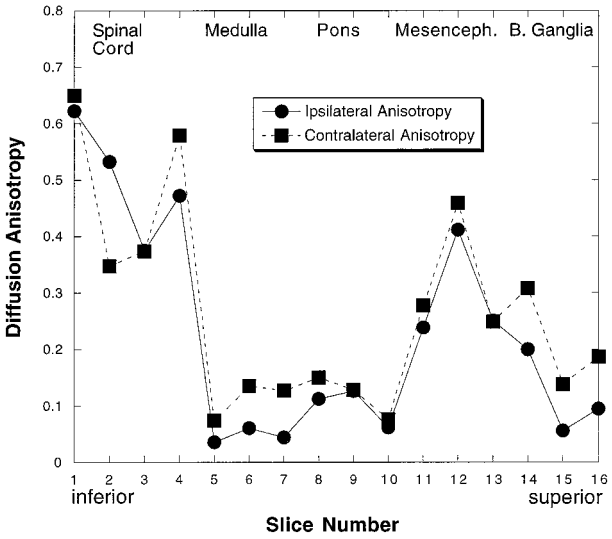

FIG 2. Diffusion anisotropy measurements following the corticospinal fiber tract in case 2. Measurements from 16 sections are shown. Sections are 5 mm thick with no gap between sections. Section 1 is the most inferior section. The diffusion anisotropy decreased bilaterally in the pons (sections 7–10) and parts of the medulla (sections 5 and 6) (see Fig 3 for the locations of the axial sections).

even when there were only small changes in T2 signal abnormality and no anatomic changes.

The diffusion anisotropy of the pons was smaller than in the rest of the CST. This may be the result of the fact that transverse pontine fibers crossed through the CST, reducing the effect of the dominant superior-inferior direction of the small-scale incoherent water motion in the measured voxels (5).

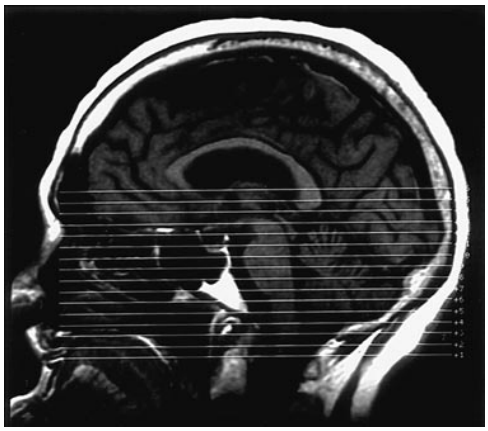

FIG 3. Sagittal MR image shows the locations of the axial sections of Figure 2.

Case 3

A 38-year-old patient with a large, right, putamenal hemorrhage was imaged 3 weeks after the event. Standard MR images (T1-weighted, FLAIR, T2-weighted, and gradient-echo) showed a subacute hematoma with associated vasogenic edema (Fig 4). Foci of hyperintensity were present on the right side of the brain stem on T2-weighted and FLAIR images, compatible with early wallerian degeneration.

Superior to the spinal cord, the average diffusion anisotropy (from 13 sections) was 0.11 in the right CST (ipsilateral to the hemorrhage) (Fig 4D) and 0.15 in the left CST, corresponding to a 24% decrease (Table 3). In the spinal cord, the average anisotropy measured from four sections was 0.31 for the ipsilateral side and 0.20 for the contralateral side, corresponding to a change of 36%.

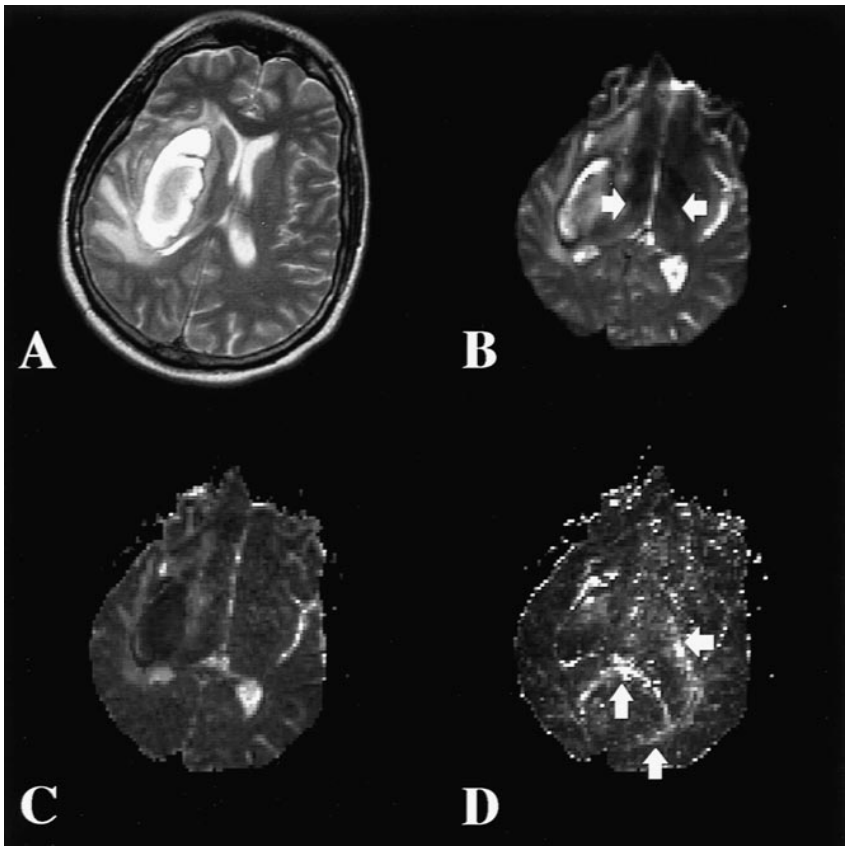

FIG 4. Case 3.

A, T2-weighted MR image shows a subacute hematoma in the right basal ganglia with associated vasogenic edema.

B, T2-weighted echo-planar image (the B_0 image from the diffusion sequence) at the next most inferior section shows the caudal edge of the hematoma. Note the slightly increased signal of the PLIC bilaterally (*arrows*).

C, An average diffusion map (D_{av}) reveals increased diffusion in the vasogenic edema adjacent to the hematoma. The right and left PLIC show no evidence of abnormal diffusion.

D, Diffusion anisotropy map (UA_{surf}) reveals hyperintensity in normal white matter tracts, including the splenium of the corpus callosum, optic radiations, and left PLIC (*arrows*). This increased signal represents the high degree of anisotropy of normal white matter tracts. The right PLIC is not visible owing to decreased anisotropy.

TABLE 3: Average (± SD) measurements following corticospinal white matter tract in patient (case 3) with early wallerian degeneration secondary to right putaminal hemorrhage 3 weeks after ictus (diffusion anisotropy index [UA_{surf}] is normalized between 0 and 1)

	Ipsilateral		Contralateral	
	D_{av} (10^{-5} cm^2/s)	UA_{surf}	D_{av} (10^{-5} cm^2/s)	UA_{surf}
Above pyramidal decussion	0.84 ± 0.20	0.11 ± 0.08	0.81 ± 0.12	0.15 ± 0.06
Spinal cord	0.94 ± 0.16	0.31 ± 0.26	0.83 ± 0.23	0.20 ± 0.09

In this case of early wallerian degeneration, the right ipsilateral CST had a lower diffusion than the contralateral side, but the change in D_{av} (4% increase) was minimal (Fig 4C). Our findings suggested that the fiber tract was damaged (anisotropy was low) and gliosis had not yet developed (D_{av} was not dramatically increased).

Case 4

A 13-year-old patient with progressive bulbar paralysis was imaged. Work-up excluded all other known causes of the clinical findings and a diagnosis of Fazio-Londe syndrome was made. Standard MR imaging findings were normal except for bilateral hypointensity on T2-weighted images in the globus pallidus, consistent with calcium or mineral deposition.

Using the diffusion-tensor imaging pulse sequence, we obtained 21 diffusion-weighted images with seven gradient directions for every MR section of 3 mm. The diffusion constant obtained from 25 measurements showed that D_{av} (1.1 ± 0.4 10^{-5} cm^2/s) was elevated, which may be consistent with gliosis that has been reported on postmortem examinations (6) in this rare disorder. The average diffusion anisotropy from 25 measurements was slightly increased ($UA_{surf} = 0.39 \pm 0.17$), perhaps a result of the thinner sections, which decrease tissue heterogeneity in the imaged voxels.

Discussion

Over the past several years, MR imaging techniques have been developed that take advantage of various biochemical and/or microscopic features of normal and pathologic tissue. In diffusion-weighted imaging, differences in self-diffusion of water molecules produce contrast between normal and pathologic tissue, in particular, acute infarctions. With this technique, the effects of the normal cellular organization of highly ordered tissues, such as white matter, can cause alterations in the rate of self-diffusion that produce changes in signal intensity on diffusion-weighted images that can be mistaken for disease processes. Therefore, the effects of tissue anisotropy are eliminated with standard diffusion-weighted imaging sequences by averaging acquisitions with diffusion-sensitive gradients applied in three directions (*x*, *y*, and *z*).

It is also possible to directly assess the effects of anisotropic diffusion. This information may be used to create maps of the direction of white matter tracts or to determine the degree of anisotropy that is present. In order to produce maps of the degree and/or the direction of anisotropy, it is necessary to obtain images with diffusion-sensitive gradients applied in more than the three directions used in routine diffusion-weighted imaging (at least six directions). Data are obtained with gradients applied singly, in pairs, and in combination (gradients applied in *x*, *y*, and *z* planes simultaneously), which allows us to calculate the direction and degree of anisotropy. By comparing the diffusion anisotropy with known normal values or with unaffected, normal portions of the same brain, it is possible to assess the degree to which tissues have maintained or lost their normal degree of organization. This technique, known as diffusion-tensor imaging, should prove to be most efficacious in evaluating processes that affect the most anisotropically ordered portions of the brain, the white matter tracts.

As we demonstrated in this series of patients, the information supplied by diffusion-tensor imaging is unique and cannot be obtained from other imaging techniques. ALS is a disease that can affect upper motor neurons, and therefore abnormalities in the CST can be detected on routine MR studies in some but not all cases. In the patient with ALS studied in this series, no abnormalities were noted on routine MR images, but a focal decrease in the extent of anisotropy in the CST was seen within the internal capsule. In the two patients with wallerian degeneration, the entire CST inferior to the area of damage had decreased anisotropy. This decrease extended caudally along the brain stem and then crossed to the contralateral spinal cord below the medullary decussation.

The fourth patient in this series, a 13-year-old, had a rare disorder known as Fazio-Londe syndrome, in which there is destruction of brain stem cranial nerve nuclei. Pathologic studies in these patients reveal neuronal loss and gliosis of the nuclei. Generalized atrophy and volume loss in the brain and spinal cord are seen less often and to a variable extent. The diffusion MR findings in our patient reflected this pathologic process. Although the routine imaging findings were normal, there was evidence of an increase in the average diffusion coefficient, suggestive of gliosis, without remarkable changes in diffusion anisotropy.

Although the ability to measure the complete diffusion tensor and to quantify diffusion anisotropy can be invaluable in determining white matter fiber tract damage, one should be aware of the limitations of this imaging method. In general, diffusion images have lower resolution and contain artifacts, such as image distortions, owing to the fact that most diffusion imaging methods use single-shot echo-planar techniques to acquire data. In our series, we found variations in the standard deviations and absolute values for diffusion anisotropy in the two cases of wallerian degeneration. Improvements

in signal-to-noise ratio and higher-resolution examinations should overcome these problems, although imaging time may increase as a consequence.

Conclusion

We believe that the use of diffusion-tensor imaging and production anisotropy maps can assist in diagnosing and determining the extent of diseases that cause fiber damage and neuronal degeneration.

References

1. Uluğ AM, Barker PB, Bryan RN, van Zijl PCM. **Diffusion tensor imaging of the human brain.** Presented at the annual meeting of the Society of Magnetic Resonance, Nice, 1995
2. Uluğ AM, Bakht O, Bryan RN, van Zijl PCM. **Mapping of human brain fibers using diffusion tensor imaging.** Presented at the annual meeting of the International Society for Magnetic Resonance in Medicine, New York, 1996
3. Uluğ AM, van Zijl PCM. **Orientation-independent diffusion imaging without tensor diagonalization: anisotropy definitions based on physical attributes of the diffusion ellipsoid.** *J Magn Reson Imaging* (in press)
4. Brooks BR. **El ESCORIAL World Federation of Neurology criteria for diagnosis of amyotrophic lateral sclerosis.** *J Neurol Sci* 1994;128(Suppl):96–107
5. Pierpaoli C, Barnett A, Virta A, Penix L, Chen R. **Diffusion MRI of wallerian degeneration: a new tool to investigate neural connectivity in vivo?** Presented at the annual meeting of the International Society for Magnetic Resonance in Medicine, Sydney, 1998;1267
6. McShane MA, Boyd S, Harding B, Brett EM, Wilson J. **Progressive bulbar paralysis of childhood: a reappraisal of Fazio-Londe disease.** *Brain* 1992;115:1889–1900